ELSEVIER

Journal of Alloys and Compounds 228 (1995) 23–30

Journal of ALLOYS AND COMPOUNDS

Mechanism of indium electrodeposition on bismuth cathodes and time evolution of the deposits

Stefano Canegallo, Vassilis Demeneopoulos*, Luisa Peraldo Bicelli, Giovanni Serravalle

Dipartimento di Chimica Fisica Applicata del Politecnico di Milano, Centro di Studio sui Processi Elettrodici del CNR, Piazza L. da Vinci, 32, 20133 Milano, Italy

Received 21 February 1995

Abstract

The mechanism of the indium electrodeposition process from aqueous solutions on bismuth cathodes has been investigated as well as the evolution with time of the composition of the deposits after electrodeposition. The potentiometric results and the changes in composition and structure are explained by considering the transport phenomena and the reactions occurring in the solid state owing to indium diffusion into the electrode and to the formation, generally, of the multiphase layer In–In_2Bi–In_5Bi_3–InBi. Such analysis allows estimation of the room temperature average diffusion coefficient of indium in the three intermetallic compounds (ca. 10^{-15}–10^{-16} m^2 s^{-1}). Moreover, consideration of the indium chemical potentials within each compound makes it possible to account for the evolution of the system with time to InBi.

Keywords: Electrodeposition; Indium; Bismuth; Intermetallic compounds; Diffusion coefficients

1. Introduction

In a recent paper [1], which followed a previous investigation [2], we studied the formation of thin InBi deposits by galvanostatic electrodeposition of In on bulk Bi cathodes at room temperature. Depending on the discharge conditions, several In–Bi intermetallic compounds (InBi, In_5Bi_3, In_2Bi) and pure In were recognised in these deposits. Owing to In diffusion and reaction inside the bulk of the electrode, the composition of the deposits changed with time, the process ending when a uniform InBi layer had been formed. The aim of this part of the research is to investigate the mechanism of this process in order to evaluate the In diffusion coefficient in the different In–Bi compounds and to suggest an interpretative model.

2. Experimental

Bi of 99.9995% purity was employed as the working electrode while the reference and counterelectrode were obtained from a 99.999% In bar. The electrolyte was 0.67 N $InCl_3$, pH 1.3. The employed current densities ranged from 2.4 to 21.4 A m^{-2} and the electrodeposition time from 1.2 to 8.3 h. All measurements were carried out at room temperature. The selected experimental conditions were such that that no parasitic hydrogen evolution took place, so that the quantity of electrodeposited In could be evaluated from the following reaction:

$$In^{3+} + 3e^- = In \quad (1)$$

More details, in particular those regarding the electrochemical apparatus (Amel, Yokogawa), the scanning electron microscope (SEM) and the energy dispersive spectrometer (EDS) (Cambridge Instrument and AN10/25-Link) as well as the X-ray diffractometer (Philips), are reported in our previous paper [1].

3. Results and discussion

Fig. 1(a) shows the open-circuit potential vs. In of the Bi electrode as a function of the circulated charge obtained by regularly opening the circuit during In electrodeposition at a constant current density. On the

* Present address: Department of Chemical Engineering, Section (III): Material Science, National Technical University, 9 Iroon Polytechniou Road, Zografou 157 73, Athens, Greece.

Elsevier Science S.A.
SSDI 0925-8388(95)01668-6

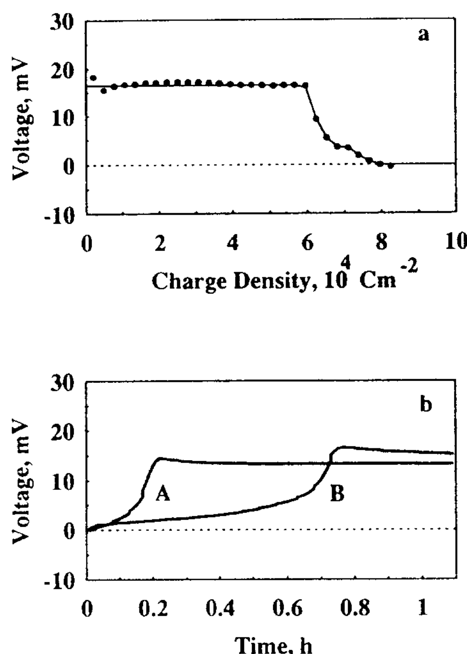

Fig. 1. (a) Open-circuit potential vs. In of the Bi cathode as a function of the charge circulated during In electrodeposition at 4.8 A m^{-2}. This is run 3 of Table 1. (b) Time dependence of the cathode potential vs. In after In electrodeposition at 7.2 A m^{-2} for 2 h (curve A) and 2.7 h (curve B). These correspond to runs 4 and 5, respectively, of Table 1.

basis of thermodynamic data (see below) and ex situ X-ray analysis [1], the potential plateau around 15 mV vs. In (average value) was related to the presence of InBi on the electrode surface, the very short one around 5 mV vs. In to In_2Bi and that at 0 mV vs. In to In, while the potential values between the plateaus were considered as mixed potentials. As expected, the time at which the electrode potential changed from one value to the other decreased with increasing current density. So, at the lowest value (1.2 A m^{-2}) In did not appear on the electrode surface even after 8.3 h deposition, whereas at the highest value (21.4 A m^{-2}) InBi was practically not observed.

After electrodeposition, the open-circuit potential increased with time up to the value for InBi (Fig. 1(b)), the final product. This singular behaviour was due to In diffusion into the bulk of the material, as observed by SEM. Indeed, the In crystals, initially covering the electrode surface, were seen to become smaller and smoother and finally to disappear. Other experimental results will be considered in the following.

3.1. Evolution during electrodeposition

The electrochemical system is given in Fig. 2. Two subsequent steps are envisaged: the In charge-transfer process according to reaction (1) and In diffusion into the InBi layer towards the InBi/Bi interface where the

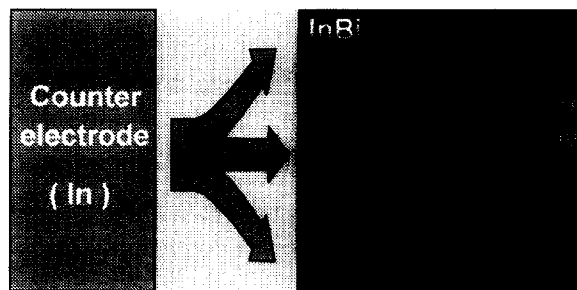

Fig. 2. Scheme of the In–Bi cell showing In^{3+} electrodeposition and In diffusion into InBi when InBi only is formed.

following reaction takes place:

$$In + Bi = InBi \qquad (2)$$

The kinetics of the first step are determined by the current density, i, which was constant in our experiments. In agreement with Faraday's law, the moles of In deposited on the unit surface area, m^*_{dep}, increased linearly with time, t:

$$m^*_{dep} = \frac{it}{zF} \qquad (3)$$

z being the number of charges transferred during the electrochemical process ($z = 3$ in our case) and F being Faraday's constant.

Schmalzried [3a,b] has already analysed the case where two metals A and B react to form the intermetallic compound A_nB_m, separated from the reactants by two phase boundaries so that the reaction proceeds by diffusion of the participating components through the reaction product. The same seems to apply to the system under investigation, where A, B and A_nB_m are In, Bi and InBi, respectively. The overall driving force for the reaction is the difference in Gibbs free energy between the reactants and the reaction product. For a very low solubility of the reactants in the reaction product, i.e. for products having a narrow range of homogeneity, the particle fluxes are locally constant. As long as the local thermodynamic equilibrium is maintained within the reaction layer and at the phase boundaries, a parabolic growth rate results, as shown in the Appendix (Eq. (18)). Consequently, the number of moles of In that may be removed from the unit surface area to form the intermetallic compound, m^*_{rem}, also shows a parabolic dependence (Eq. (19), Appendix). Comparing now the deposited and removed In quantities

$$m^*_{dep} = \frac{it}{zF} \qquad (4)$$

and

$$m^*_{rem} = \sqrt{D^*t} \qquad (5)$$

three different situations may occur:

(a) $m^*_{rem} > m^*_{dep}$, all the electrodeposited In diffuses into the cathode forming an InBi layer the growth rate of which is determined by the deposition rate, i.e. by the current density;

(b) $m^*_{rem} < m^*_{dep}$, In accumulates on the electrode surface since the diffusion and reaction process (now controlling the growth rate) is not able to remove all the electrodeposited material;

(c) $m^*_{rem} = m^*_{dep}$, the maximum possible growth rate of the layer without In surface accumulation being observed.

Fig. 3 shows the typical time dependence of both m^*_{dep} and m^*_{rem} at room temperature. m^*_{dep} depends on the electrodeposition rate and, therefore, different straight lines are obtained at the different (constant) current densities. In contrast, just one curve depicts the quantity of removed In, which depends, at constant temperature and pressure, on the material properties only (in particular the In diffusion coefficient). The intersection point of the $m^*_{rem}(t)$ curve with each of the $m^*_{dep}(t)$ straight lines gives the limiting time, t^*, above which In surface accumulation takes place, at each current density. This time may be determined from the experimental curves (e.g. Fig. 1(a)). In fact, because of the discontinuity in the experimental data of the open-circuit potential, we determined the minimum (t^*_{min}) and maximum (t^*_{max}) times, as well as the average value (t^*) at which a change in the surface composition was observed potentiometrically. At these values, the open-circuit potential vs. In decreased from the typical value for InBi towards zero, indicating a progressive surface enrichment with In. The data are presented in Table 1 together with the D^* values obtained by equating m^*_{rem} to m^*_{dep} using the following equation:

$$D^* = \left[\frac{i}{zF}\right]^2 t^* \qquad (6)$$

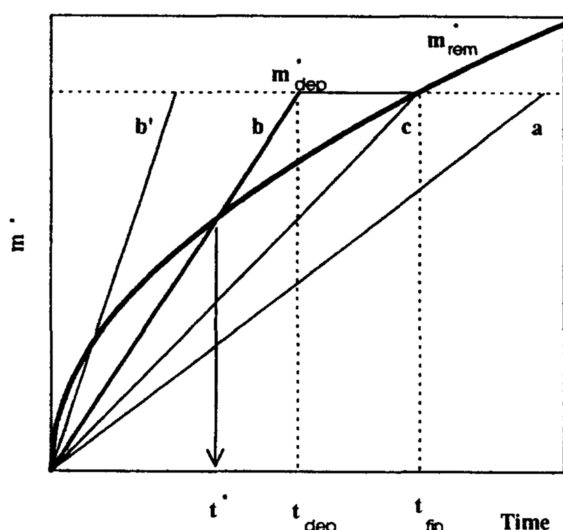

Fig. 3. Comparison at room temperature of the time dependence of the number of moles of In deposited on the unit surface at several current densities, $m^*_{dep}(t)$, (straight lines, cases a, b and c, see text) and the number of moles of In removed from the unit surface, $m^*_{rem}(t)$ (parabolic curve). In case b, the arrow indicates the time at which $m^*_{rem} = m^*_{dep}$.

Assuming for D^* the average value of runs 2–9, i.e. $D^* = 3.66 \times 10^{-6}$ mol^2 m^{-4} s^{-1}, we obtained the curve with error bars depicted in Fig. 4. For comparison, in the same figure we report the parametric curves for $D^* = 1 \times 10^{-6}$ and 1×10^{-5} mol^2 m^{-4} s^{-1}, labelled 1 and 10, respectively.

During runs 1, 10 and 11 no variation in the open-circuit potential was noted. Such a variation must occur after the last measurement of run 1 (i.e. after 8.1 h) and before the first measurement of runs 10 and 11 (i.e. before 0.32 h). Assuming our average value for D^*, we estimated these quantities as 14.8 and 0.19 h, respectively. Since D^* is related to the average In diffusion coefficient in InBi through Eqs. (19) and (18) (Appendix), we obtain (at 298 K):

$$D_{In}(InBi) \approx 1 \cdot 10^{-15}\, m^2\, s^{-1}$$

For this calculation we utilised the value of Chevalier [4] at 298 K for the InBi standard Gibbs

Table 1
Determination of the D^* value (see text)

Run	i	$Q_{min} \times 10^{-4}$	$Q_{max} \times 10^{-4}$	t^*_{min}	t^*_{max}	t^*	$D^* \times 10^6$
	(A m^{-2})	(C m^{-2})	(C m^{-2})	(h)	(h)	(h)	(mol^2 m^{-4} s^{-1})
1	2.4	7.00	—	8.10	—	>8.10	>2.00
2	4.8	5.90	6.10	3.41	3.53	3.47	3.44
3	4.8	5.90	6.10	3.41	3.53	3.47	3.44
4	7.2	3.25	3.75	1.25	1.45	1.35	3.01
5	7.2	3.25	3.75	1.25	1.45	1.35	3.01
6	10.6	2.50	3.10	0.66	0.81	0.73	3.54
7	11.9	2.40	3.20	0.56	0.75	0.65	3.98
8	11.9	2.40	3.20	0.56	0.75	0.65	3.98
9	14.3	2.40	3.30	0.47	0.64	0.55	4.86
10	21.4	—	2.50	—	0.32	<0.32	<6.38
11	21.4	—	2.50	—	0.32	<0.32	<6.38

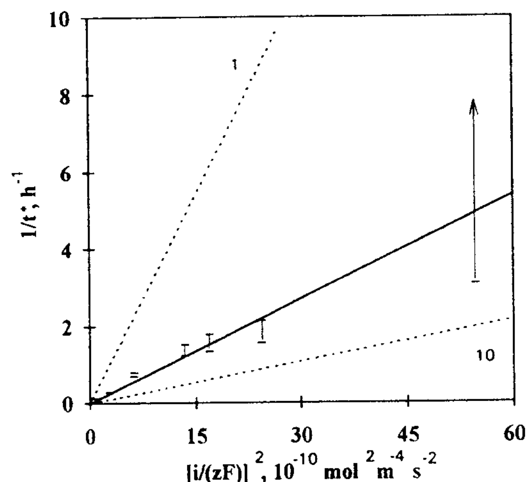

Fig. 4. Experimental $1/t^*$ values with error bars as a function of $[i/(zF)]^2$ with $D^* = 3.66 \times 10^{-6}$ mol^2 m^{-4} s^{-1}. The arrow indicates that t^*_{min} is unknown for runs 10 and 11 (see Table 1). The parametric curves with $D^* = 1 \times 10^{-6}$ and 1×10^{-5} mol^2 m^{-4} s^{-1} are labelled 1 and 10, respectively.

free energy of formation appearing in Eq. (18) (Appendix). Chevalier determined the free energies of InBi, In_5Bi_3 and In_2Bi by averaging the experimental data by different authors [5–7] and obtained at 298 K the values −3.72, −2.84 and −2.77 kJ g-atom^{-1} (of In), respectively.

Note the very high value of the In average diffusion coefficient in InBi at room temperature. Much lower values, usually between 10^{-20} and 10^{-50} m^2 s^{-1}, have been obtained for common metals and for Ge and Si [8]. However, at higher temperatures, diffusion coefficients as high as that for In in InBi may be found. For example, the In diffusion coefficient in InSb is ca. 10^{-16} m^2 s^{-1}, at 373 K [9] and that of Zn in Cu is 4×10^{-15} m^2 s^{-1} at 1007 K [8].

When the diffusion process is not able to remove all the deposited In to form InBi, the deposit may contain, in addition to InBi, In and In–Bi intermetallic compounds of composition In_nBi_m, with $n/m > 1$, as shown in Fig. 5. Indeed, In accumulating on the electrode surface may react with InBi according to the following equations:

$$\mathrm{In} + \mathrm{InBi} = \mathrm{In_2Bi} \quad (7)$$

$$\mathrm{In} + \frac{3}{2}\,\mathrm{InBi} = \frac{1}{2}\,\mathrm{In_5Bi_3} \quad (8)$$

the thermodynamic quantities for which can be evaluated from previous data. The free energy changes at 298 K of reactions (7) and (8) turn out to be −1.82 and −1.52 kJ mol^{-1}, respectively, and the related potentials to be 6.3 and 5.2 mV vs. In.

As previously stated, a short quasi-plateau around 5 mV vs. In was noted in some of the experimental curves (e.g. Fig. 1(a)). Owing to the small difference

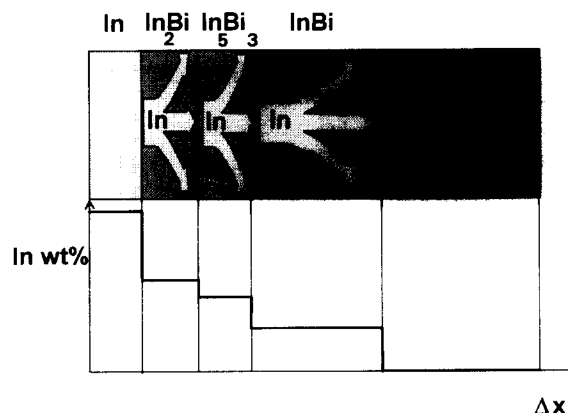

Fig. 5. Scheme of the cathode composition and of In diffusion into the In–Bi intermetallic compounds at the end of the electrodeposition process (upper part), and In wt% as a function of the deposit thickness (lower part).

between the thermodynamic values, it was not possible to determine potentiometrically which of the two reactions had occurred. The quasi-plateau was, therefore, assigned to reaction (7), since, unlike In_2Bi, In_5Bi_3 was never observed on the electrode surface by ex situ analyses [1].

3.2. Evolution after electrodeposition

3.2.1. Transition state of the system

In the most general case, the deposit was composed of In, In_2Bi, In_5Bi_3 and InBi at the end of the electrodeposition process (Fig. 5) and the composition evolved with time. The behaviour of such multiphase product layers with respect to In diffusion and reaction can be evaluated by applying to each of the individual phases the treatment given in the Appendix, provided that their range of homogeneity is sufficiently narrow and local equilibrium is maintained [3b]. This results in a parabolic growth rate (Eq. (18), Appendix) for each reaction product, and, therefore, for the total thickness of the multiphase layer. However, $\Delta\mu_{In}(In_nBi_m)$, the difference between the In chemical potential at the In_nBi_m interfaces in Eq. (18), is no longer proportional to the standard free energy of formation from the elements of In_nBi_m, as is the case when only one intermetallic compound (InBi) is formed. This difference may be calculated using the method of Schmalzried [3c], the main principles of which are as follows. The reaction product consists of a series of different phases of the type In_nBi_m (In_2Bi–In_5Bi_3–InBi), as shown in Fig. 5. Each intermetallic compound is produced at its respective right-hand interface by reaction of the diffusing species (In) with the intermetallic compound having a lower In content, whereas it is consumed at the left-hand interface by reaction with In to form the compound having a

higher In content. For example, in the case of In_5Bi_3, these reactions are given by Eqs. (8) and (9), respectively:

$$In + In_5Bi_3 = 3In_2Bi \quad (9)$$

By applying the equilibrium conditions at the two interfaces of each reaction product layer, the difference $\Delta\mu_{In}$ between the In chemical potential at each left- and right-hand boundary may be evaluated. Taking account of the values given above for the thermodynamic quantities of the In–Bi compounds, we obtain at the phase boundaries of In_2Bi:

$$\Delta\mu_{In}(In_2Bi) = \mu°(In_5Bi_3) - 3\ \mu°(In_2Bi) = 5.47 \text{ kJ g-atom}^{-1} \text{ (of In)}$$

A similar treatment for In_5Bi_3 gives:

$$\Delta\mu_{In}(In_5Bi_3) = \frac{3}{2}\mu°(InBi) - \frac{3}{2}\ \mu°(In_5Bi_3) + 3\ \mu°(In_2Bi) = -9.63 \text{ kJ g-atom}^{-1} \text{ (of In)}$$

and for InBi:

$$\Delta\mu_{In}(InBi) = -\frac{5}{2}\mu°(InBi) + \frac{1}{2}\ \mu°(In_5Bi_3) = 7.88 \text{ kJ g-atom}^{-1} \text{ (of In)}$$

where $\mu°(In_nBi_m) = \Delta G°_f(In_nBi_m)/n$.

Note that the difference in chemical potential at either side of the In_5Bi_3 layer has a negative sign whereas for In_2Bi and InBi it is positive. Therefore, In diffusion through In_5Bi_3 is not favourable, which may explain why the latter compound was never observed at the electrode surface (see below).

From the more general form of Eq. (18) (Appendix) it may be seen that so long as metallic In is present on the sample surface, the ratios of the thicknesses of the different intermetallic compounds are independent of time and given by

$$\frac{\Delta x(In_nBi_m)}{\Delta x(InBi)} = \sqrt{\frac{D_{In}(In_nBi_m) \cdot \Delta\mu_{In}(In_nBi_m)}{D_{In}(InBi) \cdot \Delta\mu_{In}(InBi)}} \quad (10)$$

where In_nBi_m refers to either In_2Bi or In_5Bi_3.

Table 2 lists the thickness, $\Delta x(In_nBi_m)$, of the layers of the different In–Bi intermetallic compounds as a function of time (columns 3–5) as well as their ratios to that of InBi (columns 6–7). Time was measured starting from the end of the electrodeposition process. Strictly speaking, the values reported in Table 2 were recorded only at 24.45 h, since In had disappeared from the electrode surface just after 24 h. However, nearly the same values were obtained after about twice that time. Introducing into Eq. (10) the value 0.28 for the ratio between the thicknesses of In_2Bi and InBi, and the average value 0.66 for that between In_5Bi_3 and InBi, together with the estimated values of $D_{In}(InBi)$ and $\Delta\mu_{In}(In_nBi_m)$ given above, we obtain for the average In diffusion coefficients (at 298 K):

$$D_{In}(In_2Bi) \approx 1 \cdot 10^{-16}\ m^2\ s^{-1}$$

$$D_{In}(In_5Bi_3) \approx 3 \cdot 10^{-16}\ m^2\ s^{-1}$$

Of course, these are first-approximation values since they were estimated from two groups of experimental data only. The In diffusion coefficient also turns out to be very high in In_2Bi and In_5Bi_3 compared with the values of other metals at room temperature (between 10^{-20} and 10^{-50} $m^2\ s^{-1}$ [8], see above).

The presence of a multiphase product layer between In and Bi allows us to explain the observed potentiometric behaviour. After electrodeposition In diffusion with reaction proceeds utilising metallic In on the deposit surface, as shown by the increasingly positive values of the potential vs. In during SEM observation of In crystals collapsing on the electrode surface and by SEM–EDS analysis of the sample surface and cross-section [1]. As soon as metallic In is no longer available at the sample surface, In_2Bi and In_5Bi_3 decompose according to the reverse of Eqs. (9) and (8), respectively, producing In. As previously shown, the chemical potential of In at the In_2Bi/In_5Bi_3 interface increases within In_5Bi_3 while that at the $In_5Bi_3/InBi$ interface decreases within InBi. Therefore, In_5Bi_3 would be expected to be more readily decomposed than In_2Bi, as was observed experimentally. Indeed, the intermediate species In_5Bi_3 was completely decomposed while In_2Bi was still present on the deposit surface. Following a similar argument, we may expect

Table 2
Total thickness (column 2), thicknesses of the individual layers of the multiphase deposit of run 11 at different times after electrodeposition (columns 3—5) and relative thicknesses to InBi (columns 6 and 7)

Time (h)	Thickness (μm)	$\Delta x(In_2Bi)$ (μm)	$\Delta x(In_5Bi_3)$ (μm)	$\Delta x(InBi)$ (μm)	$\frac{\Delta x(In_2Bi)}{\Delta x(InBi)}$	$\frac{\Delta x(In_5Bi_3)}{\Delta x(InBi)}$
0.7	15.59 ± 1.52	—	—	—	0	0
24.45	22.95 ± 1.25	3.49 ± 0.26	6.98 ± 0.42	12.48 ± 0.57	≈0.28	≈0.56
48.07	26.72 ± 1.80	3.68 ± 0.28	9.94 ± 0.70	13.10 ± 0.82	≈0.28	≈0.75
72.15	24.82 ± 1.71	2.41 ± 0.16	1.74 ± 0.60	20.67 ± 0.96	≈0.15	≈0.08
95.82	25.06 ± 0.65	2.04 ± 0.28	—	23.02 ± 0.37	≈0.08	0
339.42	24.56 ± 0.55	—	—	24.56 ± 0.55	0	0

that even during In electrodeposition In_5Bi_3 does not appear on the electrode surface, since, otherwise, the In chemical potential would strongly increase within the outermost deposit layer (of In_5Bi_3), an unfavourable condition for In diffusion. Hence, the surface would immediately be covered by In or In_2Bi. So, the assignment of reaction (7) to the quasi-plateau at 5 mV vs. In seems to be reasonable.

3.2.2. Final state of the system

In the analysed time-scale (1500 h), the evolution of the composition of the deposit was concluded with the formation of a single layer of InBi after a time depending on the deposited quantity of In. All experimental results point to this conclusion. Indeed, the average electrode potential was always ca. 15 mV vs. In. X-Ray diffraction analysis showed only peaks for InBi, while the In surface composition as studied by EDS approached asymptotically the theoretical value for InBi (35.46 wt%). SEM–EDS analysis of the sample cross-section showed a unique layer of InBi [1].

The time necessary to conclude this evolution, t_{fin}, was evaluated using the model for the behaviour during electrodeposition described in the first part of the paper. Indeed, by the end of the evolution process, all the deposited In had diffused and reacted to form InBi, and the quantity of In removed was equal to that deposited:

$$m^*_{rem} = m^*_{dep}$$

with

$$m^*_{dep} = \frac{it_{dep}}{zF} \qquad (11)$$

t_{dep} being the deposition time. As for m^*_{rem}, two cases have to be distinguished (see Fig. 3):

(1) $t_{dep} \leq t^*$ (cases (a) and (c) above). In does not accumulate on the electrode surface since the growth rate is controlled by the deposition rate, hence:

$$m^*_{rem} = \frac{it_{fin}}{zF} \qquad (12)$$

that is, $t_{fin} = t_{dep}$.

(2) $t_{dep} > t^*$ (case (b) above). The quantity of In removed follows the linear law for $t \leq t^*$ and the parabolic law for $t^* < t \leq t_{fin}$. Therefore:

$$m^*_{rem} = \frac{it^*}{zF} + \sqrt{D^* t_{fin}} - \sqrt{D^* t^*} = \frac{it_{dep}}{zF} \qquad (13)$$

$$\text{since } \frac{it^*}{zF} = \sqrt{D^* t^*} \quad \text{that is:} \quad t_{fin} = \frac{\left[\frac{it_{dep}}{zF}\right]^2}{D^*} \qquad (14)$$

which allows us to estimate t_{fin}. These values are reported in Table 3 where they are compared with experimental results. The data obtained from potential measurements refer to the time at the end of the sharp increase (Fig. 1(b)) while the SEM–EDS data refer to the time at which a constant value of the deposit thickness and In surface percentage (given in the Table as sections and surfaces, respectively) was observed. In all cases, the greater than sign (>) indicates that the process was not concluded at the reported time. Note the satisfactory agreement between the experimental results, and also that, with some exceptions, the estimated values are significantly close to the experimental ones. Throughout the calculations, we assumed that InBi only was formed. Indeed, we neglected the formation of In_2Bi and In_5Bi_3, for which the In diffusion coefficients are around one order of magnitude smaller than that for InBi. Tentatively, we repeated the calculations for each of the two compounds and obtained very much higher values than the experimental ones. This indicates that the In_2Bi and In_5Bi_3 layers were thin in comparison with the InBi layer so that In mainly diffused within InBi, in agreement with SEM–EDS results (see Table 2).

Table 3
Calculated and experimental t_{fin} values (obtained following several techniques) for runs 1–11 (see text)

Run	t_{dep} (h)	t_{fin} calculated (h)	t_{fin} potentials (h)	t_{fin}^{SEM} sections (h)	t_{fin}^{SEM} surfaces (h)
1	8.3	8.3	—	—	—
2	3.6	3.5	>3.7	—	—
3	5	6.8	>5.4	—	—
4	2	2.4	>2.2	—	—
5	2.7	4.4	>3.4	—	—
6	1.5	3.0	>2.2	—	>2
7	1.2	2.4	>1.5	—	—
8	1.8	5.4	>4.6	—	—
9	1.5	5.4	>3.3	—	—
10	1.5	12.1	>8.2	>7	>10
11	3	48.4	>63	>50	>50

4. Conclusions

During In electrodeposition on Bi cathodes, In diffuses and reacts with Bi forming overlayers of In–Bi intermetallic compounds ordered according to their relative composition. In the most general case, the sequence from the surface to the bulk of the material is In, In_2Bi, In_5Bi_3, InBi, Bi. The solid-state process continues after electrodeposition, and In_5Bi_3 and In_2Bi decompose until a layer of InBi only is formed.

From the experimental data for evolution of the deposit composition with time during and after electrodeposition, we evaluated the average In diffusion coefficients within InBi and In_2Bi and In_5Bi_3, respectively. The results are:

$$D_{In}(InBi) \approx 1 \cdot 10^{-15}\, m^2\, s^{-1}$$

$$D_{In}(In_2Bi) \approx 1 \cdot 10^{-16}\, m^2\, s^{-1}$$

$$D_{In}(In_5Bi_3) \approx 3 \cdot 10^{-16}\, m^2\, s^{-1}$$

The values show the exceptionally high mobility of In in In–Bi intermetallic compounds at room temperature and explain its singular behaviour. Moreover, we estimated the In chemical potential difference at the phase boundaries of each In_nBi_m compound of the multiphase layer. The sign of this difference allows us to explain why In_5Bi_3 was found to decompose before In_2Bi and, therefore, why it was never observed on the electrode surface.

5. Appendix

We consider the diffusion and reaction of metals A and B to form the intermetallic phase A_nB_m. In the one-dimensional case of planar diffusion in isotropic media for systems with constant electrical potential, the flux equation of the component A may be written as [3a,c]:

$$j_A = -\frac{D_A c_A}{RT} \cdot \frac{d\mu_A}{dx} \quad (15)$$

where D_A is the component diffusion coefficient, c_A the concentration, μ_A the chemical potential and x the distance from the interface to the region considered. The flux is measured relative to the crystal lattice of the solid (lattice reference system).

Generally, D_A will depend to a greater or lesser extent upon the component activities. However, in the first approximation, the average value over the reaction layer can be used, especially when the activities of A and B within the region of homogeneity of the phase A_nB_m do not vary by more than a power of ten. For intermetallic compounds with very small values of Gibbs free energy of formation from the elements (e.g. NiAl, < -100 kJ mol^{-1}) this simplification is not valid. However, this is not the case for the In–Bi intermetallic compounds (values > -4 kJ mol^{-1}).

The growth law of the reaction product can be calculated taking into account that the growth rate is directly related to the fluxes within the product layer, which follow Eq. (15). So, in the more general case of diffusion of the components A and B, the rate equation for the thickness increase of the reaction product layer, Δx, is given by:

$$\frac{d\Delta x}{dt} = \left(\frac{j_A}{n} + \frac{j_B}{m}\right) \cdot v \quad (16)$$

$v = n/c_A = m/c_B$ being the molar volume. Now, combining Eqs. (15) and (16) we obtain:

$$\frac{d\Delta x}{dt} = \left(\frac{D_A}{n} + \frac{D_B}{m}\right) \cdot \frac{\Delta G_f^0}{RT} \cdot \frac{1}{\Delta x} \quad (17)$$

where D_A and D_B are the average values of the diffusion coefficients of A and B, while, as long as the local thermodynamic equilibrium is maintained, the standard free energy of formation from the elements of A_nB_m, ΔG_f°, is equal to $n \times \Delta\mu_A$. $\Delta\mu_A$ is the difference between the chemical potential of species A at the two phase boundaries of the reaction product. Integration of the above equation yields the parabolic reaction rate law in the form:

$$\Delta x^2 = 2D't, \quad \text{with} \quad D' = -\left(\frac{D_A}{n} + \frac{D_B}{m}\right) \cdot \frac{\Delta G_f^0}{RT} \quad (18)$$

In the present case, the diffusion coefficients refer to In and Bi, and the free energy to InBi. As frequently found, one of the two diffusion coefficients is much greater than the other: only In diffused within the intermetallic compound. So, the expression for D' may be simplified since $D_{Bi} = 0$ and $n = m = 1$.

The increase during electrodeposition of the InBi layer thickness according to Eq. (18) takes place so long as In is available since no InBi layer growth is possible without a supply of In from the solution. The number of moles of In which may be removed from the unit surface area during the diffusion and reaction process, m^*_{rem}, is proportional to the deposit thickness and, therefore, to the square root of time:

$$m^*_{rem} = \Delta x \cdot \frac{\rho}{M} = \sqrt{2D't} \cdot \frac{\rho}{M} = \sqrt{D^*t} \quad (19)$$

ρ and M being the InBi mass density and molecular weight, respectively.

Acknowledgements

This work is part of the Ph.D. of S. Canegallo. V. Demeneopoulos is indebted to the Time (Erasmus) programme for a grant. The research was carried out

with the financial support of the Ministero della Università e della Ricerca Scientifica e Tecnologica.

References

[1] S. Canegallo, V. Demeneopoulos, L. Peraldo Bicelli and G. Serravalle, *J. Alloys Comp.*, *216* (1994) 149.
[2] L. Peraldo Bicelli, C. Romagnani and G. Serravalle, *Electrochim. Metal.*, *IV*, *3* (1969) 233; C. Sunseri and G. Serravalle, *Metall. Ital.*, *7/8* (1976) 373.
[3] H. Schmalzried, in *Solid State Reactions*, Academic Press, New York, 1974, (a) pp. 53–66; (b) pp. 95–97; (c) pp. 124–127.
[4] P.Y. Chevalier, *Calphad*, *12* (1988) 383.
[5] R. Boom, P.C.M. Vendel and F.R. De Boer, *Acta Metall.*, *21* (1973) 807.
[6] H.P. Singh, M.H. Rao and S. Misra, *Scripta Metal.*, *6* (1972) 621.
[7] H.P. Singh, *Thesis*, Varanasi (1972); *Scr. Metall.*, *6* (1972) 519.
[8] C.A. Wert and R.M. Thomson, *Physics of Solids*, McGraw-Hill, New York, 1970.
[9] M.C. Hobson Jr. and H. Leidheiser Jr., *Trans. Met. Soc. AIME*, *233* (1965) 482.